2025 International Conference On Rehabilitation Robotics (ICORR)
May 12-16, 2025. Chicago, IL, USA

Challenge-Based Adaptation of Exoskeleton Assistance and Gamified Biofeedback Enables Automated Gait Rehabilitation

Siddharth R. Nathella[1], Keya Ghonasgi[1], Taryn A. Harvey[1], Lena H. Ting[1,2], Kinsey R. Herrin[1,3], and Aaron J. Young[1,3] *Senior Member, IEEE*

***Abstract*— Robotic and biofeedback-assisted interventions are promising alternatives to surgical intervention and supplements for traditional physical therapy for children with gait impairments. This work utilizes a human-in-the-loop optimization strategy to adaptively modulate parameters for a lightweight robotic knee exoskeleton and biofeedback video game to maximize learning potential following the challenge point framework. We tested our approach on three able-bodied participants and one pediatric patient with genu recurvatum, a common walking pattern in children with neurological injuries. We implement a Covariance Matrix Adaptation-Evolutionary Strategy (CMA-ES) optimizer to enforce a target success rate of 70% by continuously adjusting visual biofeedback and exoskeleton assistance parameters. Our experimental results demonstrate the system's ability to maintain the target challenge level for the pediatric participant. Stance hyperextension decreased significantly from pre- to post-training trials on day 2 (9.2°) and 3 (3.2°) of the case study. Swing flexion approached the clinical target of 65° by the end of the third day. The promising optimizer performance and changes in gait kinematics validate the feasibility of autonomous parameter tuning to maximize learning potential in pediatric gait rehabilitation.**

I. INTRODUCTION

Children with neurological injuries often have walking movement disorders that impact the knee joint, with a common presentation being genu recurvatum. Genu recurvatum is characterized by knee hyperextension during the stance phase of gait and limited knee range of motion during swing phase. Typically patients with genu recurvatum hyperextend between 0° and -15° [1]. Genu recurvatum limits functional mobility and can lead to long-term joint and ligament pain [2]. Treatments include strength training of the calf and quadriceps muscles and motor control exercises [2]. In many cases, invasive treatments like surgical alterations of the bony and soft tissue elements is required [3]. Physical rehabilitation is another effective tool for treatment of genu recurvatum and similar walking impairments, but it is time-intensive, requires clinician expertise, and is physically demanding for the therapist.

This work was supported by Shriners Hospitals for Children and NIH Grant No. 1DP2HD111709-01.

[1]Siddharth R. Nathella, Keya Ghonasgi, Taryn A. Harvey, Lena H. Ting, Kinsey R. Herrin, & Aaron J. Young are with the George W. Woodruff School of Mechanical Engineering, Georgia Institute of Technology, Atlanta, GA, USA snathella@gatech.edu

[2]Lena H. Ting is also with the Wallace H. Coulter Department of Biomedical Engineering, Georgia Insitute of Technology & Emory University, Atlanta, GA, USA

[3]Kinsey R. Herrin & Aaron J. Young are with the Institute for Robotics and Intelligent Machines, Georgia Insitute of Technology, Atlanta, GA, USA

Recent research on autonomous robotic exoskeletons has shown potential for assisting gait rehabilitation by offloading the clinician's physical effort to a robotic system [4]. The addition of biofeedback has further been demonstrated to help improve outcomes and engage the participant more actively in therapy [5]. Conner & Lerner [6] showed that children using visual biofeedback with a robotic exoskeleton had higher levels of plantar flexor muscle activity compared to using the exoskeleton alone. Importantly, effective rehabilitation can only occur when the patient is learning from the interaction. Research suggests that to encourage volitional learning, the training environment should engage the participant and provide sufficient challenge to promote learning without discouraging participation [7], [8].

The challenge point framework [8] suggests that the optimal challenge level for learning a given task varies as the individual's skill increases. The nominal difficulty of the task should increase alongside skill so as to track the optimal success rate to facilitate the fastest transition from "novice" to "expert". Prior work explored this approach for stroke rehabilitation, with a video game as the task, where users self-selected a challenge level [9]. The authors found that participants settled at a 74% success rate. In a similar study, players with an approximate 70% success rate showed the most learning in a "Pong" style video game. This evidence suggests that physical rehabilitation may be encouraged and more effective if an ideal success rate is enforced (where the task is not too hard or too easy) [10]. However, the modulation of challenge may be patient-specific, task-specific, etc., and manual tuning of multi-parameter systems is infeasible [11]. Thus, automated approaches for personalizing rehabilitation systems to specified challenge levels are necessary to deploy these devices in practice.

Human-in-the-loop optimization (HILO) has been used to individually customize exoskeleton parameters, resulting in superior performance over using generic device settings [12]. Exoskeleton control policies, even with few parameters, can result in different behaviors across individuals and finding ideal parameter combinations is non-trivial. In HILO, a formal numerical optimizer looks for the control policy that best fits a particular individual by testing and evaluating different parameter combinations. Covariance Matrix Adaptation-Evolutionary Strategy (CMA-ES) [13] is a common HILO optimization framework, particularly suitable when an individual's response to the same set of parameters is expected to vary with time, such as due to motor adaptation or learning [12]. Few studies have extended HILO

2025 International Conference On Rehabilitation Robotics (ICORR) | 979-8-3503-8068-2/25/$31.00 ©2025 IEEE | DOI: 10.1109/ICORR66766.2025.11062942

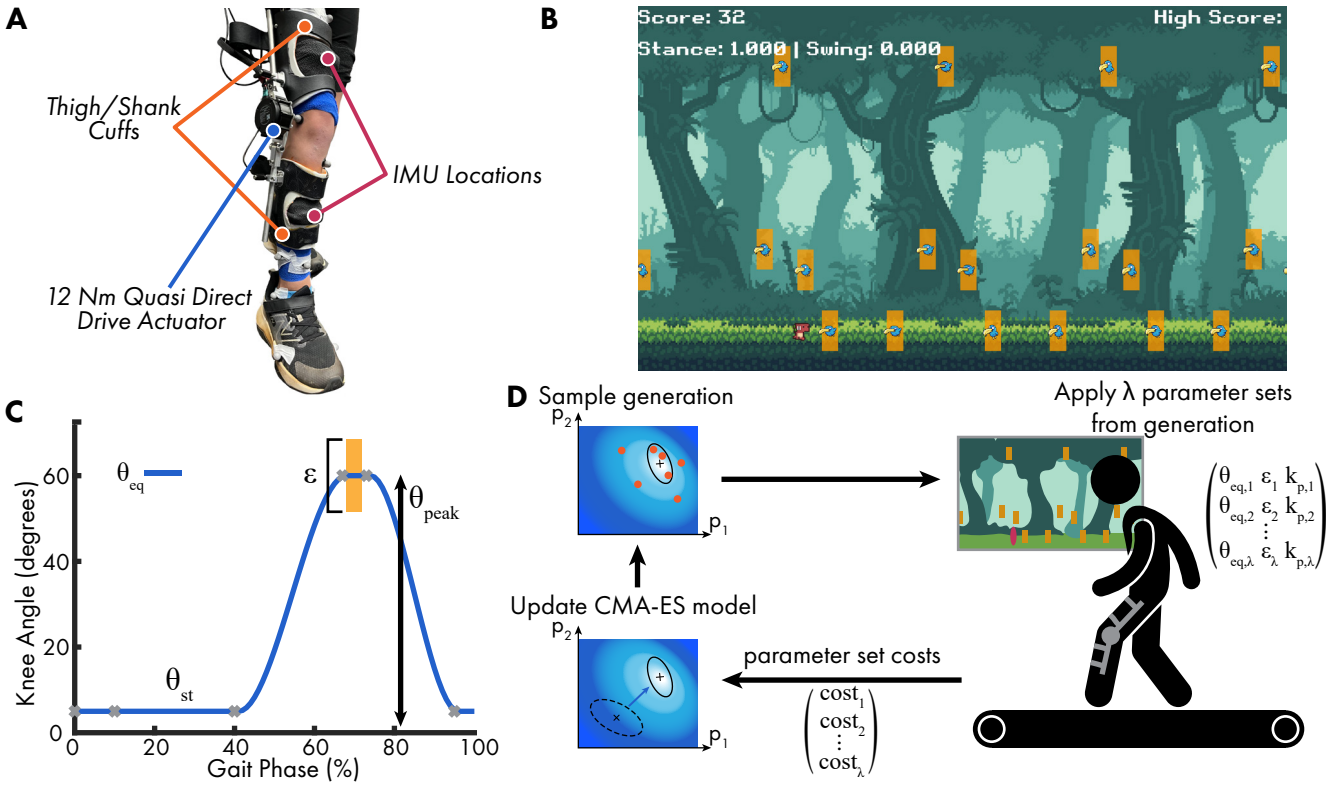

Fig. 1. (A) Knee exoskeleton designed to provide unilateral torque assistance. (B) The biofeedback video game. The red dinosaur avatar displays the user's knee angle, and the yellow boxes/birds represent the target kinematic profile for θ_{eq}, an example of which is shown in (C). The yellow box shows the tolerance factor ϵ. While the current knee angle is inside the tolerance, the assistance is set to $0\,\mathrm{Nm}$. (D) The algorithm loop to personalize gait parameters. Each CMA-ES generation applies λ parameter sets, the cost for each set is computed and used to update its estimate of the optimal region.

to rehabilitation or to motor adaptation and learning contexts. Li et al. [14] implemented HILO to encourage active voluntary participation in an upper limb movement task in stroke patients. Wang et al. [15] targeted engagement in a virtual cycling task by optimizing parameters to maximize neural engagement. This prior research and the relatively small number of studies exploring HILO for motor learning applications form the motivation for adaptively modulating challenge level, or task difficulty, to maximize the learning potential during gait training with an exoskeleton augmented by gamified biofeedback.

In this work, we formulated a knee exoskeleton and visual biofeedback system as a HILO problem to maximize learning in a walking task. We collected experimental data from three able-bodied (AB) participants challenged to walk in a crouch gait pattern, and one pediatric clinical participant with genu recurvatum (GR) prescribed to walk with a normative knee angle profile. The visual biofeedback system showed the user a goal kinematic profile in the form of a video game, while the exoskeleton applied assistive torque as needed to correct deviations from that profile. Independent stance and swing CMA-ES optimizers modified various system parameters to maintain the targeted 70% challenge level.

II. METHODS

A. Knee Exoskeleton Hardware

A lightweight ($\sim$1 kg) powered knee exoskeleton was developed to provide torque assistance to the wearer (Fig. 1A). The device assisted unilaterally, actuated by a quasi-direct drive motor (CyberGear Micromotor, Xiaomi Corp., CN), capable of $12\,\mathrm{Nm}$ of peak torque and a continuous torque of $4\,\mathrm{Nm}$. The device is an adapted version of the system in [16]. The knee joint featured a frontal plane passive degree of freedom, allowing the device to fit on individuals with deviation in frontal plane knee angles (i.e. valgus/varus). The device was secured to the participant with thermoplastic cuffs at the thigh and shank, both of which could be rotated to accommodate varying tibiofemoral transverse alignment. The device was powered by a $20\,\mathrm{V}$ off-the-shelf lithium polymer power tool battery (Dewalt, MD). A waist belt held the battery and mircrocontroller and acted to suspend the device to prevent movement during long walking sessions.

B. Knee Exoskeleton Control

The device was controlled with a Nvidia Jetson Orin Nano (Nvidia, CA) and programmed in Python 3.11. Assistance was applied using an impedance control law (Eq. 1), where the torque was defined by a stiffness parameter k_p, the measured knee angle θ_k, and an error from an equilibrium angle θ_{eq}, and an additional velocity damping term k_d, set to a constant value of $0.002\,\frac{\mathrm{Nm}}{\mathrm{deg{\cdot}s}}$. A tolerance, ϵ, was defined to set zero assistance if the error was less than ϵ, which created an assist-as-needed effect.

$$\tau = \begin{cases} 0 & |\theta_k - \theta_{eq}| \leq \epsilon \\ k_p(\theta_k - \theta_{eq}) - k_d\dot{\theta}_k & \text{else} \end{cases} \quad (1)$$

TABLE I
PARTICIPANT DEMOGRAPHIC DATA

Participant	Age	Weight (kg)	Height (cm)	Gender	Gait Pathology
AB1	28 yr	64.9	170	Male	N/A
AB2	22 yr	63.6	175	Female	N/A
AB3	24 yr	78.0	180	Male	N/A
GR1	12 yr	37.0	155	Male	*genu recurvatum*

Stance and swing optimizers use independent variables.

Knee angle was computed using two 9-axis inertial measurement units (IMU) (Microstrain by HBK, VT), placed on the thigh and shank. The difference in the roll orientation between the two sensors defined the knee angle, zeroed to a static measurement taken during quiet standing. The orientations were computed using the built-in sensor fusion algorithm. Gait phase was estimated in real-time using ground reaction forces from the treadmill, with a foot-contact threshold of $40\,\mathrm{N}$, and communicated to the controller over UDP. The estimated gait time averaged the previous two gait cycles. The controller was transitioned from stance phase into swing phase at toe-off and back to stance phase at heel contact. All control and sensing was executed at $200\,\mathrm{Hz}$.

C. Visual Biofeedback Game

The biofeedback game displayed an avatar representing the IMU measured knee angle of the participant, with targets placed along a goal kinematic trajectory (Fig. 1B). The trajectory was defined by a Piecewise Cubic Hermite Interpolating Polynomial (`pchip`), with prescriptions for stance knee angle (θ_{st}) and peak knee flexion (θ_{peak}), and all other points being interpolated. The θ_{eq} profile definition (Fig. 1C) used control points at 0, 10, 40, 67, 73, and 95% gait cycle. The game targets were displayed at 10, 40, 60, 70, and 85% gait cycle, and the target movement across the screen was aligned with the real-time estimated gait phase. The user controlled the avatar vertically on the screen, by flexing or extending their knee joint. The player received points for each target they hit and were instructed to score as many points as possible. The game was written in the Godot Game Engine (Godot Foundation) using free online assets [17], [18], [19]. The game communicated with the controller over UDP to receive real-time knee angle estimates.

D. Difficulty Adaptation Optimizer

The system was optimized using CMA-ES, a method designed to optimize black box systems by sampling and producing generations of parameter sets, ranking them by cost, and adapting its estimate of the search space. A "generation" consists of parameter sets sampled from the same search space. We selected CMA-ES based on its previous use in rehabilitation context and its suitability to time-varying spaces, but to our knowledge, this algorithm has yet to be applied in gait rehabilitation with the explicit goal of maximizing learning potential. Stance and swing phases were simultaneously optimized by independent optimizers, with the stance parameters being θ_{st}, ϵ_{st}, and $k_{p,st}$, and swing being θ_{peak}, ϵ_{sw}, and $k_{p,sw}$. Each parameter set's cost was the absolute difference between the target, 70%, and actual success rate, defined as the ratio of points scored to the total possible points over the last 10 strides of a parameter set.

$$\text{cost} = |\text{success rate} - 0.7| \tag{2}$$

For the AB participants, the bounds on θ_{st} and θ_{peak} were set to $[25, 45]^\circ$ and $[60, 85]^\circ$ respectively to challenge them to walk in a crouched posture. The bounds for the GR participant were set to $[0, 15]^\circ$ and $[45, 65]^\circ$ to encourage a normative gait profile [20], [21]. Both stance and swing bounds on ϵ were set at $\pm[1, 10]^\circ$. For the stiffness parameters, we set the maximum allowable torque to 20% of the expected peak knee moment, when the error between the current knee angle and equilibrium angle was 20°. Expected peak knee moment was taken from average kinetic profiles from literature [20], to be $0.5\,\frac{\mathrm{Nm}}{\mathrm{kg}}$ and $0.25\,\frac{\mathrm{Nm}}{\mathrm{kg}}$ for stance and swing respectively. Thus, bounds for $k_{p,st}$ and $k_{p,sw}$ were set at $[0, 0.005]\,\frac{\mathrm{Nm}}{\mathrm{deg}\cdot\mathrm{kg}}$ and $[0, 0.0025]\,\frac{\mathrm{Nm}}{\mathrm{deg}\cdot\mathrm{kg}}$. The optimizer was implemented using the `cmaes` package in Python 3.11 [22]. For the AB participants, the optimizer was configured with default recommended parameters and parameters were normalized to the recommended scaling [23]. For the GR participant, population size (λ, number of parameter sets per generation) was set to 5 instead of the default of 7. This change was made to increase the adaptation rate of the optimizer, slightly sacrificing global search performance for faster convergence, so the participant would spend more of the experiment close to the target learning rate. The effect of this change was tested using an offline bootstrapped simulation with a population size of 5. An analysis of experimental results from AB participants showed that using $\lambda = 5$ causes a shift in the next generation's estimate of each parameter by less than 10% compared to $\lambda = 7$. Given the high time cost of collecting experimental data with a pediatric subject, the smaller λ was used for this case study.

E. Experimental Protocol

We recruited N=3 able-bodied (AB) pilot subjects and N=1 pediatric genu recurvatum (GR) participant. Each visit consisted of a one-minute pre-training baseline walking trial, followed by the training session, and a one-minute post-training baseline. The primary outcome for the AB participants was optimizer performance and so they were only evaluated over one visit. The GR participant completed three visits on subsequent days to additionally evaluate knee kinematic changes. During training, the participant wore the exoskeleton and played the biofeedback game simultaneously. Every 30 seconds, a new parameter set was sampled from the CMA-ES optimizer. Once all parameter sets from a generation were trialed, the optimizer was updated (Fig. 1B). AB1 and AB3 completed 8 generations, while AB2 only completed 7 due to time restrictions. For the GR participant, 10 generations were collected each day, and the optimizer retained its state from the previous day. Kinematic data were collected using motion capture (Vicon, UK), and inverse kinematics was performed to compute joint angles (OpenSim, CA). Participants walked on a force-plate instrumented treadmill (Bertec, OH) at 80%

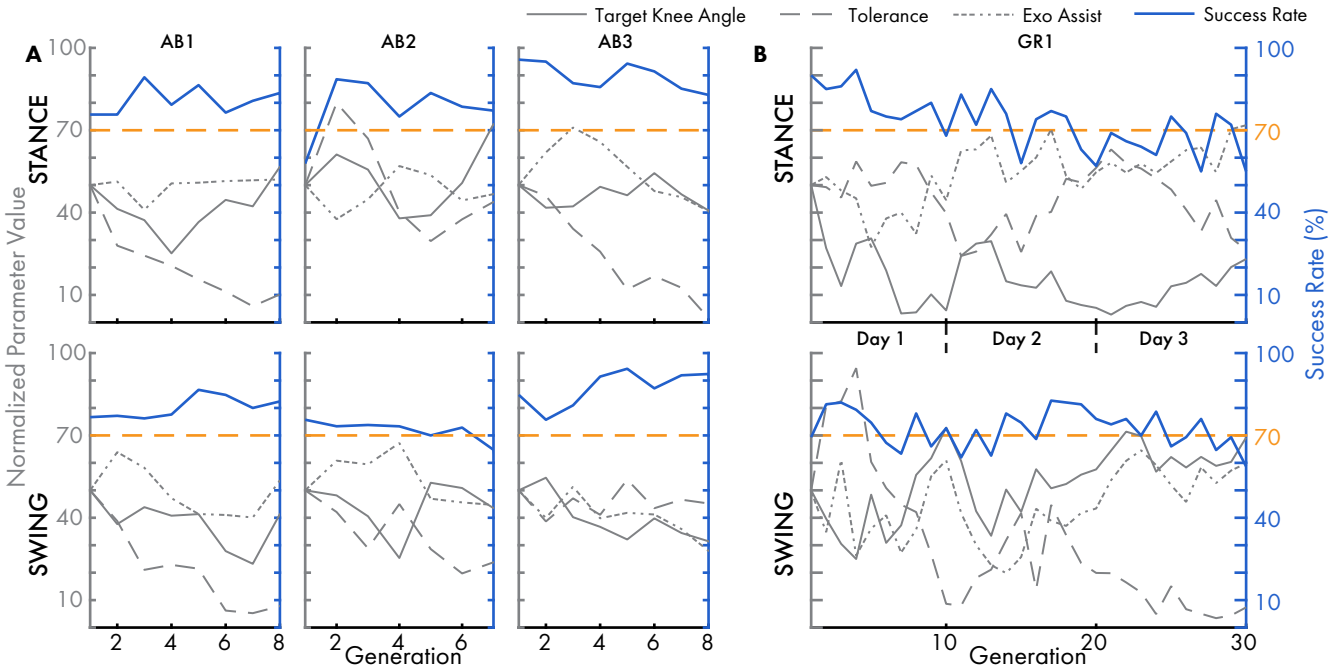

Fig. 2. Success rate and optimizer estimates over each generation for (A) AB subjects and (B) GR subjects. Blue lines denote the average success rate of each generation and grey lines denote each parameters normalized mean. Yellow dashed line marks 70% target success rate.

self-selected speed, determined through the 10-meter walk test across an instrumented gait mat (Protokinetics, PA). The AB participants took breaks as needed and breaks were enforced every 3 generations for the GR participant to minimize fatigue. The experimental protocols H19167 and H19006 were approved by the Georgia Institute of Technology Institutional Review Board.

F. Data Analysis Approach

The CMA-ES optimizer's performance was evaluated by its ability to maintain the participant's success rate at 70%. We estimated the relevance of each parameter to the optimizer by computing the variance of the optimal estimate for AB participants. High variance indicates the high relevance to maintaining the success rate. To better quantify the GR participant's responses to changes in parameters, we fit a linear model (`fitlm`, MATLAB, Mathworks, MA) comparing the inter-iteration change in parameter values (Δparam) to the change in success rate (Δsuccess rate) for each parameter. The 149 parameter set differences across three days allowed for significant correlations to be determined for this single participant. Next, we computed a personalized challenge level for each phase using a 2-norm of the set of parameters at a single iteration, where each parameter was weighted by its coefficient in the linear model, and normalized to the maximum possible challenge. Knee kinematic results were evaluated within the GR participant using one-way ANOVA with a Tukey post-hoc test to determine significant changes between conditions (`multcompare`).

III. RESULTS

A. Optimizer Performance

1) Able-Bodied Subjects: AB1 and AB3 showed a relatively high performance in the task both during stance and swing, with the optimizer being unable to pull either subject to 70% success rate by the end of the session. The optimizer was more successful with AB2, with stance phase ending within 10% of the target success rate, and achieving the target success rate during swing within 5 generations (Fig. 2A). During stance phase, for all AB participants, the target tolerance parameter selected by the optimizer consistently varied the most. For swing phase, we saw similar results for AB1 and AB2, with tolerance being the most varied parameter. In AB3, the peak knee flexion angle and exoskeleton assistance were varied more by the optimizer.

2) Pediatric Genu Recurvatum Subject: The CMA-ES optimizer was able to maintain the targeted score rate for the GR participant (Fig. 2B). During stance we saw a decreasing trend towards the 70% target, coming to within 10% of the target by the end of day 1. This target was maintained on subsequent days with mean success rates of 72% and 66.2% on days 2 & 3 respectively. The swing phase score rate started and remained close to the target across all days, with mean success rates of 73.4%, 74%, and 70.27% on days 1, 2, and 3 respectively. The stance optimizer varied all three parameters to a similar extent across the three days, whereas the swing optimizer primarily varied the tolerance parameter.

B. Score Rate Changes and Challenge for GR Participant

The swing phase score rate model identified tolerance as the only significant parameter ($p \ll 0.001$) and the others are excluded from the challenge level estimation. The knee angle and tolerance parameters were significant factors ($p \ll 0.001$) affecting stance phase score rate (Table II). The challenge level estimated from these parameters (Fig. 3) shows a strong increasing trend in swing and a soft increasing trend in stance ($p \ll 0.001$).

TABLE II

PARAMETER IMPORTANCE: (*:$p < 0.05$)

Δsuccess rate $= \beta_0 + \beta_1 \Delta\theta_{st/peak} + \beta_2 \Delta\epsilon_{st/sw} + \beta_3 \Delta k_{p,st/sw}$		
	Δstance success rate	Δswing success rate
β_0	0.0384	0.1119
β_1	3.3265*	-1.6403
β_2	4.8127*	5.0875*
β_3	1.6784	0.1668
stance challenge$_i$ $= \left\| \begin{bmatrix} \beta_1 \theta_{st,i} \\ \beta_2 \epsilon_{st,i} \end{bmatrix} \right\|_2$		swing challenge$_i$ $= \epsilon_{st,i}$

C. Kinematic Outcomes for GR Participant

Knee kinematic results were compared during the pre-training and post-training baseline conditions, as well as the last generation (5 parameter sets) on each visit for the GR participant (Fig. 4A, Section II-F). For knee hyperextension (stance phase), significant improvements between pre-training and the last generation of training were seen on all visits ($4.3°$, $7.3°$, $7.5°$ on days 1, 2, and 3 respectively, $p < 0.05$). Significant improvement between the pre- and post-training was seen on days 2 ($9.2°$) & 3 ($3.2°$) (Fig. 4B). During swing flexion, we set $65°$ as a reference, because that was the maximum target the system could show the participant. The day 1 pre-training baseline had the lowest peak knee flexion and in each subsequent condition, peak knee flexion exceeded the $65°$ reference. We saw significant changes in peak knee flexion (Fig. 4C) and, at the end of the last day, the participant was closest to the $65°$ reference.

IV. DISCUSSION

In this work, we demonstrate a HILO approach to customize exoskeleton and biofeedback parameters to maintain a specified level of success during a task. Through an experimental study, we 1) establish the efficacy of an adaptive algorithm for challenge modulation, 2) quantify parameter importance identified from the algorithm's estimations, and 3) evaluate the effects of the exoskeleton-biofeedback framework on joint kinematics. Our results from a pilot experiment with three AB participants and a clinical case study with a pediatric participant with GR provide promising evidence for simultaneous exoskeleton and biofeedback modulation to target kinematic adaptation for gait rehabilitation.

The CMA-ES algorithm showed limited ability to match the desired score rate in AB participants, despite increasing task difficulty. They could easily achieve the crouch gait with a high success rate, rendering parameters needed for a 70% success rate outside the set parameter bounds. The algorithm was more successful for the pediatric participant, as walking with a normative gait was more challenging due to their GR. The parameters required to keep the GR participant at the 70% success rate changed over time suggesting the participant was improving. An optimization strategy that cannot account for a dynamic environment (such as human adaptation) like Bayesian Optimization or Gradient Descent would not track changes in optimal parameters. Our results indicate a need for a time-varying algorithm like CMA-ES. A potential limitation of CMA-ES is the time of convergence. Some approaches to address this limitation include shrinking search spaces and faster adaptation rates.

The parameter importance computed from the sampled parameter sets suggests that target tolerance was the most important parameter for both stance and swing optimizers. A decrease in tolerance requires more precise knee motion to hit the kinematic targets, thus requiring increased volitional control over the knee joint. For the GR participant, a higher knee flexion target was associated with lower success rates in swing phase, but an increase in stance flexion target lowered the challenge of the task. This likely stems from compensatory crouch gait behavior that individuals with GR often use to avoid hyper-extension. A target stance angle close to $0°$ could not be met using crouch gait resulting in lower score rate due to lack of precise volitional control. Thus, the stance knee angle target had a similar effect as tolerance, forcing the participant toward precise knee joint control to prevent hyperextension. In stance, the exoskeleton assistance parameter was near-significance ($p = 0.0519$) and further experimental analysis is necessary to verify whether this parameter is important in participants with more severe impairment or different impairments, such as crouch gait.

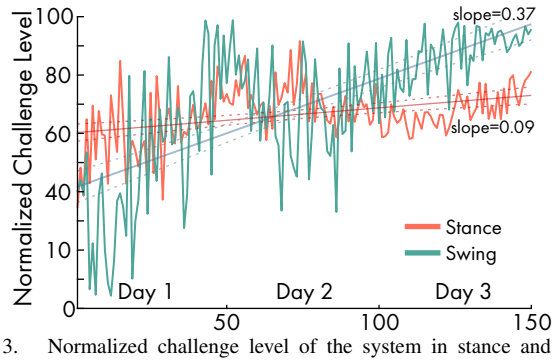

Fig. 3. Normalized challenge level of the system in stance and swing phase over each iteration for the GR subject. Both conditions trend towards higher challenge levels by the end of the experiment.

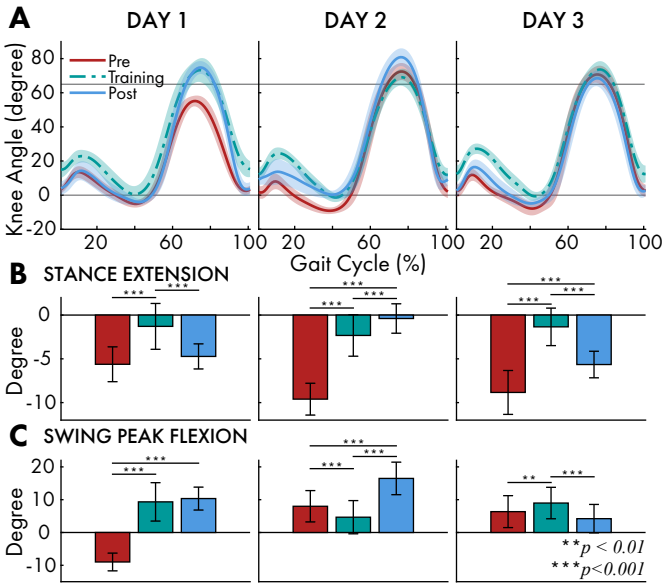

Fig. 4. (A) Knee profiles for the GR subject from (red) pre-, (teal) last generation, and (blue) post-training. (B) Minimum stance extension. (C) Peak swing flexion difference from $65°$. Error bars and shaded areas: ± 1 standard deviation.

In swing, the changes in exoskeleton assistance did not significantly change the success rate. However, there was a significant positive correlation ($R^2 = 0.44$) between the optimal peak knee flexion angle and exoskeleton assistance that the optimizer estimated (Fig. 2B). This correlation suggests that for the optimizer to maintain the intended success rate, increases in the peak knee flexion parameter must be accompanied by increases in exoskeleton assistance. In other words, the participant may have relied on the device to achieve more challenging knee flexion targets consistently. Future versions of the optimizer could be tuned to limit over-utilization of the device over the course of rehabilitation to ensure users receive maximal carryover benefit.

The exoskeleton and biofeedback system affected immediate changes in gait kinematics toward the target behaviors, with some evidence for retention across days. Although the pediatric participant exhibited exaggerated peak swing flexion (i.e. steppage gait) on the first and second days going beyond the target of 65°, on day 3, this exaggeration was less severe. This trend suggests the participant adapted to the desired behaviors over time despite initial overcompensation. In stance phase, hyperextension improved during training on all visits, with carryover from pre- to post-training on days 2 and 3. Both these kinematic outcomes could be negatively affected by a limitation of the visual biofeedback game which only rewards meeting the knee angle targets. As the game does not explicitly penalize hyperextension during stance or exaggerated flexion during swing it may inadvertently reinforce compensatory behaviors. Future versions of the game will incorporate such penalties alongside positive rewards.

The long-term goal of this research is to encourage gait rehabilitation in pediatric patients with gait impairments such as genu recurvatum and crouch gait. The able-bodied pilot and pediatric clinical case study presented in this paper are a first step toward this goal. Future work in this direction should aim to further evaluate different adaptation algorithms, their effect on a larger population and more diverse set of impairments, and the efficacy of adaptive training for long-term rehabilitation. The current study and ongoing improvements in the design and control of exoskeletons and serious games highlight the promising potential of adaptive training protocols for gait retraining through autonomous modulation of task difficulty to encourage learning.

ACKNOWLEDGMENT

We thank our participants for their time. We also thank Emily Rice, Dennis Green, Arina Kucinskaja, and Antonio Garcia Jimenez for their help during data collections.

REFERENCES

[1] D. A. Yngve, "Recurvatum of the Knee in Cerebral Palsy: A Review," *Cureus*, vol. 13, p. e14408, Apr. 2021.

[2] J. K. Loudon, H. L. Goist, and K. L. Loudon, "Genu Recurvatum Syndrome," *Journal of Orthopaedic & Sports Physical Therapy*, vol. 27, pp. 361–367, May 1998. Publisher: Journal of Orthopaedic & Sports Physical Therapy.

[3] R. S. Dean, N. R. Graden, D. H. Kahat, N. N. DePhillipo, and R. F. LaPrade, "Treatment for Symptomatic Genu Recurvatum: A Systematic Review," *Orthopaedic Journal of Sports Medicine*, vol. 8, p. 2325967120944113, Aug. 2020. Publisher: SAGE Publications Inc.

[4] D. Lee, M. K. Shepherd, S. C. Mulrine, J. D. Schneider, K. F. Moore, E. M. Eggebrecht, B. M. Rogozinski, K. R. Herrin, and A. J. Young, "Reducing Knee Hyperextension With an Exoskeleton in Children and Adolescents With Genu Recurvatum: A Feasibility Study," *IEEE Transactions on Biomedical Engineering*, vol. 70, pp. 3312–3320, Dec. 2023.

[5] T. C. Bulea, Z. F. Lerner, A. J. Gravunder, and D. L. Damiano, "Exergaming with a pediatric exoskeleton: Facilitating rehabilitation and research in children with cerebral palsy," in *2017 International Conference on Rehabilitation Robotics (ICORR)*, pp. 1087–1093, July 2017. ISSN: 1945-7901.

[6] B. C. Conner and Z. F. Lerner, "Improving Ankle Muscle Recruitment via Plantar Pressure Biofeedback during Robot Resisted Gait Training in Cerebral Palsy," in *2022 International Conference on Rehabilitation Robotics (ICORR)*, pp. 1–6, July 2022. ISSN: 1945-7901.

[7] J. A. Kleim and T. A. Jones, "Principles of experience-dependent neural plasticity: implications for rehabilitation after brain damage," *Journal of speech, language, and hearing research: JSLHR*, vol. 51, pp. S225–239, Feb. 2008.

[8] M. A. Guadagnoli and T. D. Lee, "Challenge point: a framework for conceptualizing the effects of various practice conditions in motor learning," *Journal of Motor Behavior*, vol. 36, pp. 212–224, June 2004.

[9] Q. Sanders, V. Chan, R. Augsburger, S. C. Cramer, D. J. Reinkensmeyer, and A. H. Do, "Feasibility of Wearable Sensing for In-Home Finger Rehabilitation Early After Stroke," *IEEE Transactions on Neural Systems and Rehabilitation Engineering*, vol. 28, pp. 1363–1372, June 2020.

[10] N. Al-Fawakhiri, S. Kayani, and S. D. McDougle, "Evidence of an optimal error rate for motor skill learning," July 2023. Pages: 2023.07.19.549705 Section: New Results.

[11] K. Ghonasgi, R. Mirsky, S. Narvekar, B. Masetty, A. M. Haith, P. Stone, and A. D. Deshpande, "Capturing Skill State in Curriculum Learning for Human Skill Acquisition," in *2021 IEEE/RSJ International Conference on Intelligent Robots and Systems (IROS)*, pp. 771–776, Sept. 2021. ISSN: 2153-0866.

[12] P. Slade, C. Atkeson, J. M. Donelan, H. Houdijk, K. A. Ingraham, M. Kim, K. Kong, K. L. Poggensee, R. Riener, M. Steinert, J. Zhang, and S. H. Collins, "On human-in-the-loop optimization of human–robot interaction," *Nature*, vol. 633, pp. 779–788, Sept. 2024. Publisher: Nature Publishing Group.

[13] N. Hansen, "The CMA Evolution Strategy: A Comparing Review," in *Towards a New Evolutionary Computation: Advances in the Estimation of Distribution Algorithms* (J. A. Lozano, P. Larrañaga, I. Inza, and E. Bengoetxea, eds.), pp. 75–102, Berlin, Heidelberg: Springer, 2006.

[14] N. Li, Y. Yang, T. Yang, W. Chen, Y. Wang, P. Yu, W. Wang, N. Xi, and L. Liu, "Human-in-the-loop Optimization for Adaptive Assist-as-Needed Rehabilitation," in *2022 12th International Conference on CYBER Technology in Automation, Control, and Intelligent Systems (CYBER)*, pp. 1050–1054, July 2022. ISSN: 2642-6633.

[15] J. Wang, W. Wang, S. Ren, W. Shi, and Z.-G. Hou, "Engagement Enhancement Based on Human-in-the-Loop Optimization for Neural Rehabilitation," *Frontiers in Neurorobotics*, vol. 14, Nov. 2020. Publisher: Frontiers.

[16] D. Lee, S. Lee, and A. J. Young, "AI-driven universal lower-limb exoskeleton system for community ambulation," *Science Advances*, vol. 10, p. eadq0288, Dec. 2024.

[17] "Dino Character Sprites by Arks." https://arks.itch.io/dino-characters.

[18] "Pixel Adventure 2 by Pixel Frog." https://pixelfrog-assets.itch.io/pixel-adventure-2.

[19] "Jungle Asset Pack by Jesse Munguia." https://jesse-m.itch.io/jungle-pack.

[20] M. H. Schwartz, A. Rozumalski, and J. P. Trost, "The effect of walking speed on the gait of typically developing children," *Journal of Biomechanics*, vol. 41, pp. 1639–1650, Jan. 2008.

[21] J. Camargo, A. Ramanathan, W. Flanagan, and A. Young, "A comprehensive, open-source dataset of lower limb biomechanics in multiple conditions of stairs, ramps, and level-ground ambulation and transitions," *Journal of Biomechanics*, vol. 119, p. 110320, Apr. 2021.

[22] M. Nomura and M. Shibata, "cmaes : A Simple yet Practical Python Library for CMA-ES," Oct. 2024. arXiv:2402.01373.

[23] N. Hansen, "The CMA Evolution Strategy: A Tutorial," 2016. Publisher: arXiv.